Koch, *Proc. Natl. Acad. Sci. U.S.A.* **88**, 11569 (1991)] have indicated that membrane conductance can increase by a factor of 10.
15. The main (parvocellular) input to the monkey cortex is remarkably linear, exhibiting neither response amplitude saturation nor response phase advance. Magnocellular inputs in the monkey, however, show both strong amplitude saturation and prominent response phase advance [R. M. Shapley, *Annu. Rev. Psychol.* **41**, 635 (1990); E. A. Benardete, E. Kaplan, B. W. Knight, *Visual Neurosci.* **8**, 483 (1992)]. Our prediction of a fourfold increase in conductance is based on the assumption that inputs from the LGN are themselves linear. If simple cells receive significant magnocellular input this assumption is wrong, and we are overestimating the dependence of conductance on stimulus contrast.
16. N. J. Berman, R. J. Douglas, K. A. C. Martin, and D. Whitteridge [*J. Physiol. (London)* **440**, 697 (1991)] measured only slight conductance increases for a drifting bar stimulus. However, a drifting bar is a weak stimulus; stimulus energy is formally defined as the integral of the power spectrum (the Fourier energy) of the stimulus. Our model predicts that a stronger stimulus (like a full contrast drifting grating) would yield a larger increase in conductance. Even so, our model predicts that conductance increases in their experiment by a factor of 1.5, which is significantly greater than the factor of 1.2 they reported.
17. B. Jagadeesh, H. S. Wheat, and D. Ferster [*Science* **262**, 1901 (1993)] found that fluctuations in membrane potential evoked by drifting grating stimuli were accurately predicted by a linear model. Our model misestimates the membrane potential fluctuations in their experiment by a factor of 1.2 ± 0.2, depending on the cell's semisaturation contrast.
18. We thank J. A. Movshon for generous support and advice. We also thank H. B. Barlow, E. J. Chichilnisky, S. DuLac, and D. Baylor for helpful comments and C. Tang and L. P. O'Keefe for helping us collect the data. Some of this research was presented in abstract form at the Association for Research in Vision and Ophthalmology Annual Meeting (1993), the European Conference on Visual Perception (1993), and the Society for Neuroscience Annual Meeting (1993). Supported by Consiglio Nazionale delle Ricerche (Italy), by National Institute of Mental Health grant 1-R29-MH50228-01, and by NASA grant NCC2-307.

8 December 1993; accepted 19 April 1994

An Increased Percentage of Long Amyloid β Protein Secreted by Familial Amyloid β Protein Precursor (βAPP_{717}) Mutants

Nobuhiro Suzuki,* Tobun T. Cheung,* Xiao-Dan Cai, Asano Odaka, Laszlo Otvos Jr., Christopher Eckman, Todd E. Golde, Steven G. Younkin†

Normal processing of the amyloid β protein precursor (βAPP) results in secretion of a soluble 4-kilodalton protein essentially identical to the amyloid β protein (Aβ) that forms insoluble fibrillar deposits in Alzheimer's disease. Human neuroblastoma (M17) cells transfected with constructs expressing wild-type βAPP or the βAPP_{717} mutants linked to familial Alzheimer's disease were compared by (i) isolation of metabolically labeled 4-kilodalton Aβ from conditioned medium, digestion with cyanogen bromide, and analysis of the carboxyl-terminal peptides released, or (ii) analysis of the Aβ in conditioned medium with sandwich enzyme-linked immunosorbent assays that discriminate $A\beta_{1-40}$ from the longer $A\beta_{1-42}$. Both methods demonstrated that the 4-kilodalton Aβ released from wild-type βAPP is primarily but not exclusively $A\beta_{1-40}$. The βAPP_{717} mutations, which are located three residues carboxyl to $A\beta_{43}$, consistently caused a 1.5- to 1.9-fold increase in the percentage of longer Aβ generated. Long Aβ (for example, $A\beta_{1-42}$) forms insoluble amyloid fibrils more rapidly than $A\beta_{1-40}$. Thus, the βAPP_{717} mutants may cause Alzheimer's disease because they secrete increased amounts of long Aβ, thereby fostering amyloid deposition.

The 39– to 43–amino acid polypeptide Aβ, deposited as amyloid (*1*, *2*) in the brains of patients with Alzheimer's disease (AD), is derived from a set of 677 to 770 amino acid proteins collectively referred to as βAPP (*2*–*4*). Strong evidence that amyloid deposition plays a critical role in the development of AD has come from the identification of familial AD (FAD) kindreds in which the AD phenotype cosegregates with mutations in the βAPP gene. Three of the FAD-linked βAPP mutations convert the valine located three residues carboxyl to $A\beta_{43}$ (Val^{717} in βAPP_{770}) to isoleucine (ΔI) (*5*), phenylalanine (ΔF) (*6*), or glycine (ΔG) (*7*). A fourth double mutation (ΔNL) alters the lysine-methionine located immediately amino to $A\beta_1$ (Lys^{670}-Met^{671} in βAPP_{770}) to asparagine-leucine (*8*). The location of these mutations immediately suggests that they may cause AD by altering βAPP processing in a way that is amyloidogenic.

Cells expressing $\beta APP_{\Delta NL}$ secrete five to six times more 4-kD Aβ than those expressing wild-type βAPP (*9*, *10*). Thus, $\beta APP_{\Delta NL}$ undergoes altered processing that enhances the likelihood of amyloid deposition. Transfected cells expressing $\beta APP_{695\Delta I}$ do not, however, release increased amounts of Aβ (*9*). To account for this observation, we proposed (*9*) that the FAD-linked mutations on the carboxyl side of Aβ (ΔI, ΔF, ΔG) shift cleavage to favor generation of longer Aβs such as $A\beta_{1-42}$ or $A\beta_{1-43}$. Because these longer Aβs form amyloid fibrils more rapidly than $A\beta_{1-40}$ (*11*, *12*), shifting the site of cleavage could result in amyloid deposition without increasing the overall amount of Aβ produced. Here we have used two different methods to test this hypothesis.

Our initial approach was to label transfected M17 cells with [^{35}S]methionine plus either [^{3}H]valine or [^{3}H]isoleucine. The radioactively labeled Aβ in conditioned medium was then separated by immunoprecipitation and tris-tricine SDS–polyacrylamide gel electrophoresis (PAGE) as previously described (*13*), transferred to immobilon, visualized autoradiographically, and excised. The excised 4-kD Aβ was digested with cyanogen bromide (CNBr), which cleaves Aβ on the carboxyl side of the methionine at $A\beta_{35}$, releasing COOH-terminal peptides beginning at $A\beta_{36}$ (for example, $A\beta_{36-40}$ from $A\beta_{1-40}$, $A\beta_{36-42}$ from $A\beta_{1-42}$). Finally, the radiolabeled CNBr peptides were separated by reversed-phase liquid chromatography (RPLC) with a Vydac narrow bore C4 column. CNBr digestion was carried out in the presence of excess unlabeled $A\beta_{36-40}$ and $A\beta_{36-42}$ both to improve recovery of the labeled COOH-terminal peptides and to mark, by ultraviolet absorbance, the fractions in which $A\beta_{36-40}$ and $A\beta_{36-42}$ elute.

The radioactively labeled COOH-terminal peptides that CNBr releases from the 4-kD Aβ produced by M17-βAPP_{695} cells labeled with [^{35}S]methionine plus [^{3}H]valine are shown in Fig. 1A. The major radiolabeled peptide eluted from the C4 column with unlabeled $A\beta_{36-40}$. In addition, there was minor labeled peptide that eluted with unlabeled $A\beta_{36-42}$ (*14*). To further characterize these COOH-terminal peptides, we examined the large amount of 4-kD Aβ released from M17-$\beta APP_{695\Delta NL}$ cells labeled with [^{35}S]methionine plus either [^{3}H]valine or [^{3}H]isoleucine (Fig. 1B). We identified the major COOH-terminal peptide released from this 4-kD Aβ by CNBr digestion as $A\beta_{36-40}$ by (i) radiosequencing it to show valine residues at positions 1 and 4 as expected (*15*), (ii) demonstrating (Fig. 1B) that it is not labeled by [^{3}H]isoleucine and therefore terminates be-

N. Suzuki and A. Odaka, Discovery Research Division, Takeda Chemical Industries, Ltd., Wadai 10, Tsukuba, Ibaraki, 300-42 Japan.
T. T. Cheung, X.-D. Cai, C. Eckman, T. E. Golde, S. G. Younkin, Division of Neuropathology, Institute of Pathology, Case Western Reserve University, Cleveland, OH 44106, USA.
L. Otvos Jr., The Wistar Institute of Anatomy and Biology, Philadelphia, PA 19104, USA.

*These authors contributed equally to this study.
†To whom correspondence should be addressed.

fore the isoleucine at position 41, and (iii) showing that it coelutes from the C4 column with unlabeled synthetic $A\beta_{36-40}$ (Fig. 1A) and not with $A\beta_{36-39}$ (*16*). Thus, most of the 4-kD Aβ released by our transfected M17 cells ends at $A\beta_{40}$. It is clear, however, that the minor radiolabeled peptide shown in Fig. 1, A and B, represents longer Aβ extending beyond position 40. This peptide was labeled by [^{3}H]isoleucine (Fig. 1B), and radiosequencing showed that the isoleucine was at position 6 as expected for a CNBr-generated COOH-terminal peptide beginning at $A\beta_{36}$ and extending through the isoleucine at position 41. Thus, a fraction of the 4-kD Aβ released by our transfected M17 cells is long Aβ extending through $A\beta_{41}$ (*14*), and this longer Aβ can be evaluated by examination of the COOH-terminal peptide released from it by CNBr digestion.

To evaluate the effect of the ΔI mutation on the production of long Aβ under circumstances where there would be abundant Aβ to analyze, we compared M17 cells expressing $\beta APP_{695\Delta NL}$ (Fig. 1C) with M17 cells expressing βAPP_{695} that contained both the ΔNL and ΔI mutations ($\beta APP_{695\Delta NL+I}$) (Fig. 1D) (*17*). Quantitative comparison by phosphorimaging of the transfected M17 lines expressing $\beta APP_{695\Delta NL}$ or $\beta APP_{695\Delta NL+I}$ showed reduced βAPP expression in the ΔNL+I line and that, in this particular transfection, the ΔNL+I line released 67% less 4-kD Aβ than the ΔNL line. Consistent with this observation, the ΔNL+I line showed a 58% reduction in the major COOH-terminal $A\beta_{36-40}$ peptide released from the 4-kD Aβ that it produced. However, this line showed almost no reduction in the minor COOH-terminal peptide released from the longer Aβ within the 4-kD Aβ that it generated. Quantitation of these data showed that long Aβ constituted 5% of the Aβ produced by the ΔNL line and 11% of the Aβ produced by the ΔNL+I line. Thus, the relative amount of long Aβ produced from the ΔNL+I mutant was 2.1 times that produced from the ΔNL mutant.

To further examine this shift toward long Aβ, we retransfected M17 cells to produce new $\beta APP_{695\Delta NL}$ or $\beta APP_{695\Delta NL+I}$ lines. Quantitative phosphorimaging of the labeled Aβ produced by these new lines showed that they were releasing essentially the same amount of 4-kD Aβ. In our initial assessment of the long Aβ produced by these lines, we used a completely different approach based on sandwich enzyme-linked immunosorbent assays (ELISAs) that discriminate synthetic $A\beta_{1-40}$ from $A\beta_{1-42}$. The detection of known amounts of synthetic $A\beta_{1-40}$ or $A\beta_{1-42}$ by these sandwich ELISAs is illustrated in Fig. 2A. In both ELISAs, a monoclonal antibody (mAb) to $A\beta_{1-16}$ (BAN-50) (*18*) was used for capture. When mAb BC-05, which was raised to $A\beta_{35-43}$, was used for detection, $A\beta_{1-42}$ was recognized but $A\beta_{1-40}$ produced no signal. In contrast, when mAb BA-27 (*18*), which was raised to $A\beta_{1-40}$, was used for detection, $A\beta_{1-40}$ was recognized but $A\beta_{1-42}$ produced no signal. When the Aβ released from the ΔNL and ΔNL+I lines was compared with these two sandwich ELISAs (Fig. 2B), the M17 cells expressing $\beta APP_{695\Delta NL+I}$ showed a marked increase in the signal detected by the BAN-50/BC-05 ELISA selective for $A\beta_{1-42}$. Thus, this method also showed a shift toward long Aβ. It is evident (Fig. 2B) that the percentage of long Aβ measured by sandwich ELISA was much higher than that measured by radioactive labeling. This could well reflect poor recovery of COOH termini from long Aβ after labeling, but additional data are clearly needed to resolve this issue. Quantitation of the sandwich ELISA data showed that long Aβ constituted 19% of the Aβ produced by the ΔNL line and 31% of the Aβ produced by the ΔNL+I line. Thus, the relative amount of long Aβ produced from the ΔNL+I mutant was 1.6 times that

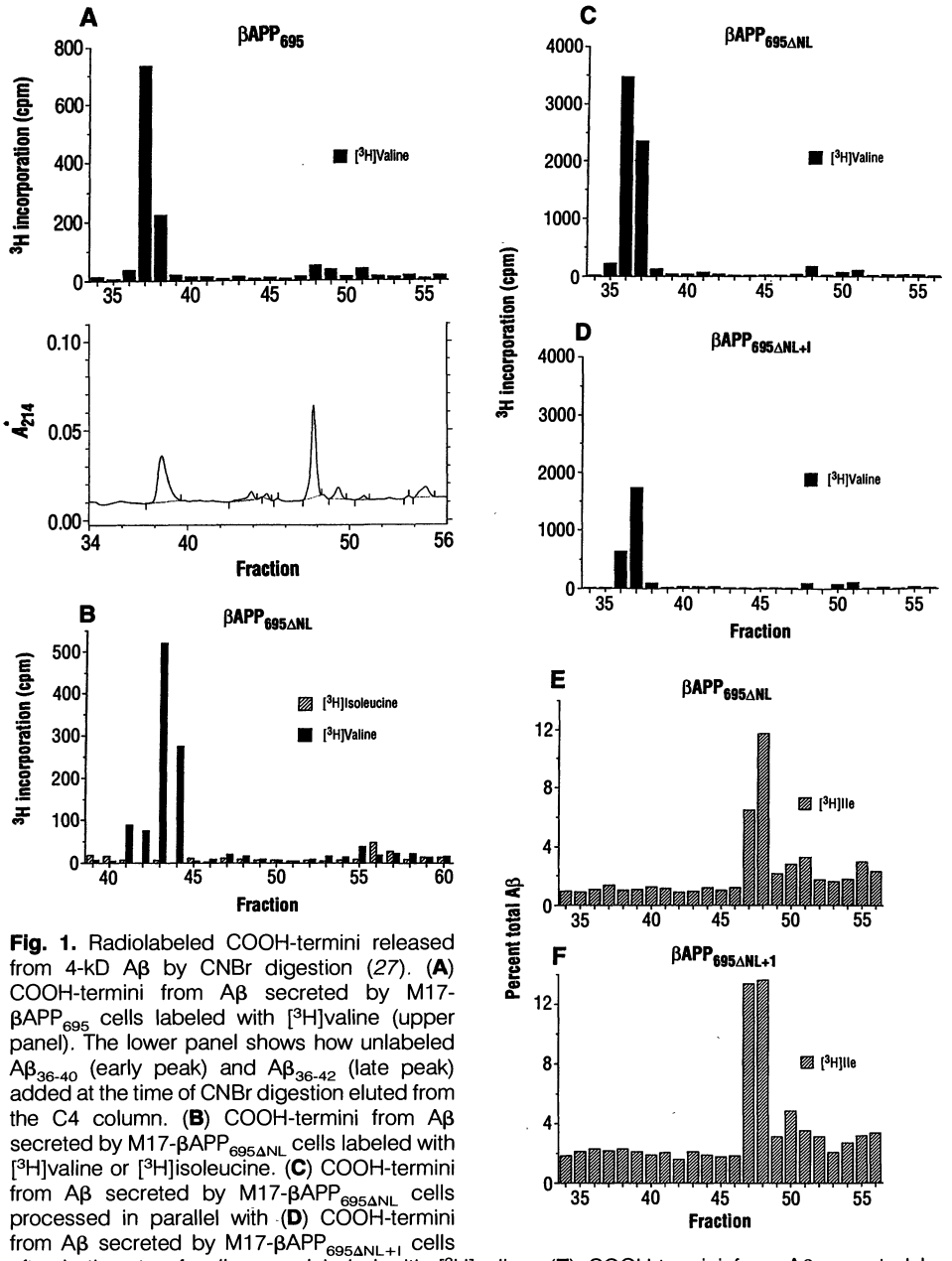

Fig. 1. Radiolabeled COOH-termini released from 4-kD Aβ by CNBr digestion (*27*). (**A**) COOH-termini from Aβ secreted by M17-βAPP_{695} cells labeled with [^{3}H]valine (upper panel). The lower panel shows how unlabeled $A\beta_{36-40}$ (early peak) and $A\beta_{36-42}$ (late peak) added at the time of CNBr digestion eluted from the C4 column. (**B**) COOH-termini from Aβ secreted by M17-$\beta APP_{695\Delta NL}$ cells labeled with [^{3}H]valine or [^{3}H]isoleucine. (**C**) COOH-termini from Aβ secreted by M17-$\beta APP_{695\Delta NL}$ cells processed in parallel with (**D**) COOH-termini from Aβ secreted by M17-$\beta APP_{695\Delta NL+I}$ cells after both sets of cells were labeled with [^{3}H]valine. (**E**) COOH-termini from Aβ secreted by M17-$\beta APP_{695\Delta NL}$ cells analyzed in parallel with (**F**) COOH-termini from Aβ secreted by M17-$\beta APP_{695\Delta NL+I}$ cells after both sets of cells were labeled with [^{3}H]isoleucine. Note (i) that the marked reduction in [^{3}H]valine-labeled COOH-termini recovered in (B) as compared with (C) reflects poor transfer to immobilon in the experiment shown in (B) and (ii) that the transfected cells examined in (E) and (F) are different from those in (C) and (D), as explained in the text.

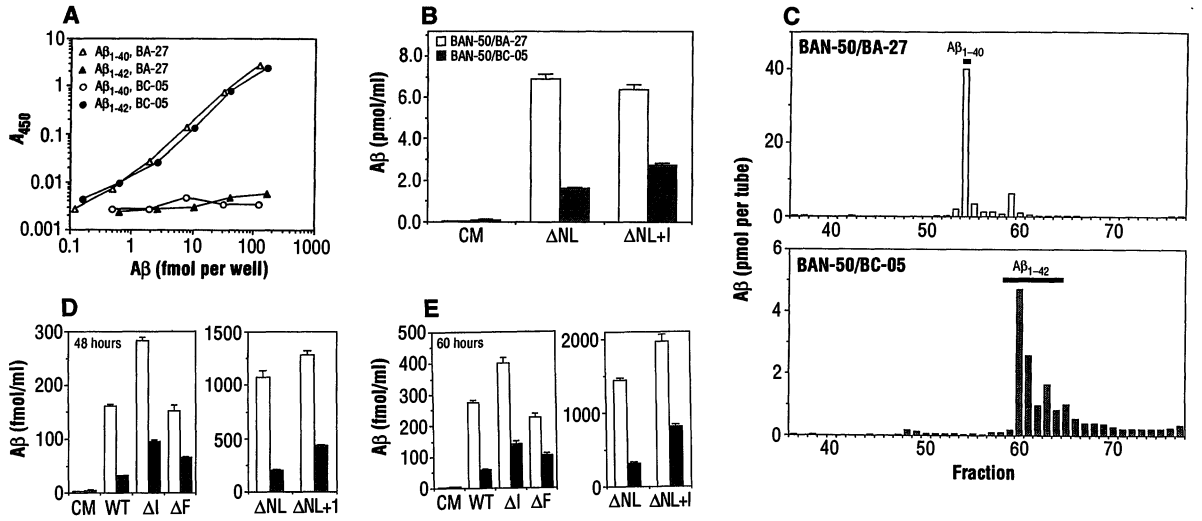

Fig. 2. Analysis by sandwich ELISA of the Aβ secreted from transfected M17 cells expressing mutant or wild-type βAPP_{695} (*28*). (**A**) Dose-response curves for synthetic $A\beta_{1-40}$ (△) or $A\beta_{1-42}$ (▲) in a BAN-50/BA-27 sandwich ELISA and for $A\beta_{1-40}$ (○) or $A\beta_{1-42}$ (●) in a BAN-50/BC-05 sandwich ELISA. (**B**) Aβ in unconditioned control medium (CM) and in medium conditioned with M17-$\beta APP_{695\Delta NL}$ (ΔNL) or M17-$\beta APP_{695\Delta NL+I}$ (ΔNL+I) cells. Cells grown to confluence in 10-cm dishes were used to condition 7 ml of medium (OPTI-MEM, 5% calf serum) for 48 hours. Aβ was analyzed in triplicate by BAN-50/BA-27 (open bars) or BAN-50/BC-05 (shaded bars) ELISA. Values shown are the mean ± SE. (**C**) Analysis by reverse-phase HPLC of the Aβ secreted from M17-$\beta APP_{695\Delta NL+I}$ cells. Confluent cells were used to condition medium (OPTI-MEM, 5% calf serum, 7 ml per 10-cm dish) for 48 hours. Conditioned medium (50 ml) was applied to a BAN-50 column consisting of 0.75 mg of the antibody immobilized to 0.1 g of Tresyl Toyopearl resin. Adsorbed materials were eluted with 1 ml of 60% CH_3CN containing 0.2% TFA, and the eluate was lyophilized and further fractionated by reverse-phase HPLC on a Vydac C4 column (4.6 by 250 mm). In the elution, CH_3CN concentration (containing 0.1% TFA) was kept at 23.75% for the first 5 min and then linearly increased from 23.75 to 32.75% over 60 min at a flow rate of 0.5 ml/min. Samples from fractions were analyzed by BAN-50/BA-27 (upper panel) or BAN-50/BC-05 (lower panel) ELISA. Horizontal bars show the fractions in which synthetic $A\beta_{1-40}$ or $A\beta_{1-42}$ eluted in control experiments. (**D** and **E**) Aβ secreted by transfected M17 cells expressing wild-type βAPP_{695} (WT) or βAPP_{695} with the FAD-linked ΔI, ΔF, ΔNL, or ΔNL+I mutations. Subconfluent cells growing to confluence in 10-cm dishes over a 48-hour period were used to condition 7 ml of medium (serum-free OPTI-MEM) for 48 (D) or 60 (E) hours. Aβ in the conditioned media or fresh culture medium (CM) was analyzed in triplicate by BAN-50/BA-27 (open bars) or BAN-50/BC-05 (shaded bars) ELISA. Values shown are the mean ± SE. Note that the marked reduction in the amount of Aβ secreted in (D) and (E) as compared with (B) is due to the omission of 5% calf serum from the medium in the experiments shown in (D) and (E). We have observed repeatedly this effect of omitting calf serum.

produced from the ΔNL mutant.

To better characterize the Aβ detected by the sandwich ELISAs described above, we used a BAN-50 column to affinity purify the Aβ in 50 ml of medium conditioned with M17-$\beta APP_{695\Delta NL+I}$ cells, then separated the affinity-purified Aβ by RPLC using a C4 column and analyzed each of the relevant fractions with the two sandwich ELISAs (Fig. 2C). The BAN-50/BC-05 assay detected only long Aβ that eluted from the C4 column at the same time as synthetic $A\beta_{1-42}$ and did not detect the major $A\beta_{1-40}$ species that eluted earlier. In contrast, the BAN-50/BA-27 ELISA detected only the major $A\beta_{1-40}$ species and a minor, as yet unidentified species that eluted immediately before the long Aβ recognized by BC-05. Thus, the increase in the BAN-50/BC-05 signal observed in medium conditioned with the $\beta APP_{695\Delta NL+I}$ as compared with the $\beta APP_{695\Delta NL}$ cells does, in fact, reflect a shift toward long Aβ.

To further validate the results obtained by sandwich ELISA, we analyzed the long Aβ produced by the new ΔNL and ΔNL+I lines with the radioactive labeling methodology described above and labeled cells with [^{3}H]isoleucine in order to focus on the COOH-terminal peptide released from long Aβ. This analysis showed that more long COOH termini were recovered from the Aβ produced by the new ΔNL+I line (Fig. 1F) than from the Aβ produced by the new ΔNL line (Fig. 1E). Quantitation of these data showed that the relative amount of long Aβ produced from the ΔNL+I mutant was 1.5 times that produced from the ΔNL mutant, a result essentially identical to the 1.6-fold increase measured by sandwich ELISA. A second assessment of the two new lines after labeling with [^{3}H]valine gave essentially identical results (Table 1). The fact that these two very different methods show essentially the same shift toward production of long Aβ in the ΔNL+I line constitutes strong evidence that the ΔI mutation does, in fact, favor production of long Aβ.

To evaluate the long Aβ produced from the naturally occurring FAD-linked βAPP_{717} mutants (ΔI and ΔF), we used the BAN-50/BC-05 and BAN-50/BA-27 ELISAs to compare the Aβ released from transfected M17 cells expressing wild-type βAPP_{695}, $\beta APP_{695\Delta I}$, or $\beta APP_{695\Delta F}$. In addition, we reexamined the Aβ produced by the new $\beta APP_{695\Delta NL}$ and $\beta APP_{695\Delta NL+I}$ lines. After 60 hours of conditioning (Fig.

Table 1. Effect of ΔI and ΔF mutations on long Aβ.

Experiment	Transfection	Percent long Aβ in 717 mutant/ percent long Aβ in control		
		Method	Comparison	Ratio
1	1	Radiolabeling	695NL + I/695NL	2.1
2	2	Sandwich ELISA	695NL + I/695NL	1.6
3	2	Radiolabeling	695NL + I/695NL	1.5
4	2	Radiolabeling	695NL + I/695NL	1.6
5 (48 hours)	2	Sandwich ELISA	695NL + I/695NL	1.6
5 (60 hours)	2	Sandwich ELISA	695NL + I/695NL	1.6
6	2	Sandwich ELISA	695NL + I/695NL	1.5
5 (48 hours)	3	Sandwich ELISA	695Ile/695WT	1.5
5 (60 hours)	3	Sandwich ELISA	695Ile/695WT	1.5
5 (48 hours)	3	Sandwich ELISA	695Phe/695WT	1.9
5 (60 hours)	3	Sandwich ELISA	695Phe/695WT	1.8
6	3	Sandwich ELISA	695Phe/695WT	1.8

Table 2. Summary of sandwich ELISA analysis. Parentheses enclose the number of separate cultures analyzed.

βAPP expressed	Percent long Aβ (mean ± SE)
βAPP_{695WT} (3)	17.5 ± 0.5
$\beta APP_{695\Delta F}$ (3)	31.4 ± 0.6*
$\beta APP_{695\Delta I}$ (2)	25.7 ± 0.5**
$\beta APP_{695\Delta NL}$ (4)	17.0 ± 1.0
$\beta APP_{695\Delta NL+I}$ (4)	26.7 ± 1.8***
All controls (WT and ΔNL) (7)	17.2 ± 0.6
All ΔI (ΔI and ΔNL + I) (6)	26.4 ± 1.2*
All 717 (ΔI, ΔF, and ΔNL + I) (9)	28.0 ± 1.1*

*P = 0.0001 **P = 0.001 ***P = 0.003 versus relevant control.

2E), the long Aβ released from wild-type βAPP_{695} was 18% of the total, and this increased to 27% for $\beta APP_{695\Delta I}$ and 32% for $\beta APP_{695\Delta F}$. The long Aβ released from $\beta APP_{695\Delta NL}$ was 18% of the total (the same percentage observed for wild-type βAPP_{695}), and this increased to 28% for $\beta APP_{695NL+I}$ (essentially the same percentage observed with $\beta APP_{695\Delta I}$). After 48 hours of conditioning (Fig. 2D), the medium bathing all lines contained less Aβ, but the percentage of long Aβ produced from controls and the shifts toward long Aβ in the ΔI, ΔF, and ΔNL+I mutants were essentially identical to those observed at 60 hours. Examination of a third set of media conditioned with the βAPP_{695}, $\beta APP_{695\Delta F}$, $\beta APP_{695\Delta NL}$, or $\beta APP_{695\Delta NL+I}$ lines gave essentially identical results.

The results of all experiments analyzing the effect of the ΔI and ΔF mutations on long Aβ are summarized in Table 1. To compare the shift toward long Aβ produced by these mutations in each experiment, we divided the percentage of long Aβ produced by the ΔI or ΔF mutant by the percentage of long Aβ produced by the relevant control. Overall, our comparison of multiple transfected cell lines expressing wild-type βAPP_{695} or the ΔI, ΔF, ΔNL, or ΔNL+I mutants by two completely different methods showed that the ΔI and ΔF mutations consistently produce a 50 to 90% shift in the relative amount of long Aβ produced. The increased percentage of long Aβ secreted by cells expressing βAPPs with the ΔI or ΔF mutations was statistically significant as shown by the data summarized in Table 2 ($P < 0.004$ by Student's t test for all comparisons made). Studies by Lansbury and his colleagues (*12*) indicate that amyloid formation is a nucleation-dependent polymerization. This type of seeded polymerization can be extremely concentration dependent. $A\beta_{1-42}$ and $A\beta_{1-43}$ nucleate very rapidly compared to $A\beta_{1-40}$ (*11*, *12*) and can seed aggregation of $A\beta_{1-40}$ in vitro (*12*). Thus, relatively subtle (50 to 90%) increases in production of long Aβ could substantially increase amyloid deposition in the decades preceding the development of dementia in patients with βAPP_{717} mutations.

The complex pathology observed in AD can be caused by trisomy 21 (*19*), the FAD-linked βAPP mutations, or by mutation of a locus on chromosome 14 (*20*). In addition, there is evidence that the ApoE4 allele substantially increases the risk of AD (*21*), and it is clear that the disease develops in many patients in which the aforementioned genetic factors play no role. Thus, AD is a heterogeneous disorder in which pathology can be initiated or accelerated by a number of genetic or environmental factors. If amyloid deposition is a rate-limiting element within a serial cascade of age-related pathologic changes that produce AD, then all factors linked to the disease will either foster amyloid deposition or enhance pathology that is provoked by amyloid. The likelihood of amyloid deposition is enhanced by trisomy 21, where there is an extra copy of the βAPP gene (*2*, *3*) and increased expression of βAPP [which is normally processed to secreted Aβ] by $\beta APP_{\Delta NL}$ [which increases secretion of 4-kD Aβ sixfold in cultured cells (*9*, *10*)], and by the βAPP_{717} mutations [which enhance secretion of highly amyloidogenic long Aβ in cultured cells]. Collectively, these findings strongly favor the hypothesis that amyloid deposition is a critical element in the development of AD, but they do not preclude the possibility that other age-related changes associated with this disease (for example, paired helical filaments) may develop in parallel and contribute to dementia independently of amyloid deposition. Thus, it will be important to continue to test the "amyloid hypothesis" by determining whether factors such as the chromosome 14 mutation and the ApoE4 allele enhance amyloidogenesis or pathology that is produced by amyloid deposition.

Note added in proof: In an immunocytochemical study with BA-27 and BC-05, Iwatsubo *et al.* (*Neuron*, in press) examined brains from (i) sporadic AD patients, (ii) Down syndrome patients, and (iii) two demented patients with the $\beta APP_{\Delta I}$ mutation. In all cases BC-05 labeled more plaques than BA-27, and it labeled them more intensely. In excellent agreement with our results, the brains from the patients with the $\beta APP_{\Delta I}$ mutation had the largest area covered by BC-05–stained plaques and the greatest preponderance of BC-05 as compared to BA-27–stained plaques.

REFERENCES AND NOTES

1. G. G. Glenner and C. W. Wong, *Biochem. Biophys. Res. Commun.* **122**, 1131 (1984); C. L. Masters *et al.*, *Proc. Natl. Acad. Sci. U.S.A.* **82**, 4245 (1985); D. J. Selkoe, C. R. Abraham, M. B. Podlisny, L. K. Duffy, *J. Neurochem.* **46**, 1820 (1986); F. Prelli, E. Castano, G. G. Glenner, B. Frangione, *ibid.* **51**, 648 (1988).
2. J. Kang *et al.*, *Nature* **325**, 733 (1987).
3. D. Goldgaber, M. I. Lerman, O. W. McBride, U. Saffiotti, D. C. Gajdusek, *Science* **235**, 877 (1987); R. E. Tanzi *et al.*, *ibid.*, p. 880; N. K. Robakis *et al.*, *Lancet* i, 384 (1987).
4. G. Konig *et al.*, *J. Biol. Chem.* **267**, 10804 (1992).
5. A. Goate *et al.*, *Nature* **349**, 704 (1991); S. Naruse *et al.*, *Lancet* **337**, 978 (1991); K. Yoshioka *et al.*, *Biochem. Biophys. Res. Commun.* **178**, 1141 (1991); J. Hardy and D. R. Group, *Lancet* **337**, 1342 (1991).
6. J. Murrell, M. Farlow, B. Ghetti, M. D. Benson, *Science* **254**, 97 (1991).
7. M.-C. Chartier-Harlin *et al.*, *Nature* **353**, 844 (1991).
8. M. Mullan *et al.*, *Nature Genet.* **1**, 345 (1992).
9. X.-D. Cai, T. E. Golde, S. G. Younkin, *Science* **259**, 514 (1993).
10. M. Citron *et al.*, *Nature* **360**, 672 (1992).
11. C. Hilbich, B. Kisters-Woike, J. Reed, C. L. Masters, K. Beyreuther, *J. Mol. Biol.* **218**, 149 (1991); D. Burdick *et al.*, *J. Biol. Chem.* **267**, 546 (1992).
12. J. T. Jarrett and P. T. Lansbury Jr., *Cell* **73**, 1055 (1993); J. T. Jarrett, E. P. Berger, P. T. Lansbury Jr., *Biochemistry* **32**, 4693 (1993).
13. M. Shoji *et al.*, *Science* **258**, 126 (1992).
14. Collectively, our radiolabeling and sandwich ELISA data provide strong evidence that the 4-kD Aβ released from transfected M17 cells is composed primarily of $A\beta_{1-40}$ and contains some longer $A\beta_{1-42}$. That some $A\beta_{1-42}$ is released is indicated by (i) our identification of COOH-termini released from 4-kD Aβ that radiosequencing shows to extend through the isoleucine at position 41 and that coelute from C4 columns with unlabeled $A\beta_{36-42}$, and (ii) our demonstration that the BAN-50/BC-05 sandwich ELISA does not recognize $A\beta_{1-40}$ and does recognize a species that coelutes from C4 columns with $A\beta_{1-42}$. In some experiments, the COOH-termini released from longer Aβ appeared to be heterogeneous, suggesting that some Aβ might extend to or beyond $A\beta_{1-43}$. To examine this possibility, we labeled transfected M17 cells expressing $\beta APP_{695\Delta NL}$ or $\beta APP_{695\Delta NL+I}$ with [^{3}H]threonine or (for the purpose of comparison) [^{35}S]methionine. Because there are no threonines in $A\beta_{1-42}$, any 4-kD Aβ labeled by [^{3}H]threonine must extend to or beyond the threonine at $A\beta_{43}$. Analysis of the ~105-kD NH_2-terminal derivative secreted by these cells showed that [^{3}H]threonine was well incorporated into βAPP, but 4-kD Aβ, separated by 10-16% tris-tricine SDS-PAGE and then dried, visualized, excised, and completely digested to optimize counting of [^{3}H]threonine, showed no signal above background. These negative data do not, of course, eliminate the possibility that a minute fraction of 4-kD Aβ may extend to or beyond $A\beta_{1-43}$. They do, however, reinforce our conclusion that most long Aβ is $A\beta_{1-42}$. Our findings are consistent with the results of Dovey *et al.* (*22*), who used an immunoaffinity approach to isolate the Aβs released from transfected 293 cells expressing $\beta APP_{\Delta NL}$, separated the Aβ by C4 high-performance liquid chromatography (HPLC), and then analyzed the resultant fractions by sandwich ELISA and mass spectrometry. This

group found $A\beta_{1-40}$ to be the major species released, showed that a small fraction was $A\beta_{1-42}$, and detected no Aβ extending past $A\beta_{42}$. This group also identified small amounts of shorter species ($A\beta_1$ to $A\beta_{28,33,34,37,38, \text{ or } 39}$) that could not be analyzed by the methods used in our study.

15. The fractions eluted from the C4 column that contained putative radiolabeled $A\beta_{36-40}$ also contained coeluting unlabeled $A\beta_{36-40}$ that had been added at the time of CNBr digestion. The unlabeled $A\beta_{36-40}$ in these fractions was sequenced at the same time that putative $A\beta_{36-40}$ was radiosequenced. As expected for $A\beta_{36-40}$, definite [^{3}H]valine signals were obtained on cycles 1 and 4. We did not obtain a definite signal for the terminal [^{3}H]valine, but this was explained by the behavior of unlabeled $A\beta_{36-40}$ which, as expected, showed a substantial reduction in yield to almost undetectable levels for the terminal valine released on the fifth cycle.
16. T. T. Cheung and S. G. Younkin, unpublished observations.
17. To assemble CEP4β-$\beta APP_{695\Delta NL+I}$, we used the ECO RI–Xba I fragment from BSKS-$\beta APP_{695\Delta I}$ (325 bp) to replace the corresponding fragment from BSKS-$\beta APP_{695\Delta NL}$. The region containing mutations was then sequenced to confirm that both mutations were present. The Hind III–Not I fragment of the resultant BSKS-$\beta APP_{695\Delta NL+I}$ was then subcloned into C4β.
18. N. Suzuki *et al.*, *Am. J. Pathol.*, in press.
19. A. H. Ropper and R. S. Williams, *Neurology* **30**, 639 (1980); D. M. A. Mann, P. O. Yates, B. Marcyniuk, C. R. Ravindra, *Neuropathol. Appl. Neurobiol.* **12**, 447 (1986).
20. G. D. Schellenberg *et al.*, *Science* **258**, 668 (1992); C. Van Broeckhoven *et al.*, *Nature Genet.* **2**, 335 (1992); M. Mullan *et al.*, *ibid.*, p. 340; P. St George Hyslop *et al.*, *ibid.*, p. 330.
21. M. Pericak-Vance *et al.*, *Am. J. Hum. Genet.* **48**, 1034 (1991); W. J. Strittmater *et al.*, *Proc. Natl. Acad. Sci. U.S.A.* **90**, 8098 (1993); E. H. Corder *et al.*, *Science* **261**, 921 (1993); D. E. Schmechel *et al.*, *Proc. Natl. Acad. Sci. U.S.A.* **90**, 9649 (1993); A. M. Saunders *et al.*, *Neurology* **43**, 1467 (1993); D. S. Borgaonkar *et al.*, *Lancet* **342**, 625 (1993); J. Poirier *et al.*, *ibid.*, p. 697; A. M. Saunders *et al.*, *ibid.*, p. 710; S. Noguchi, K. Murakami, N. Yamada, *ibid.*, p. 737; J. Hardy *et al.*, *ibid.*, p. 737; H. Payami, J. Kaye, L. L. Heston, T. D. Bird, G. D. Schellenberg, *ibid.*, p. 738; N. Anwar, S. Lovestone, M. E. Cheetham, R. Levy, J. F. Powell, *ibid.*, p. 1038; G. Lucotte *et al.*, *ibid.*, p. 1309; C. Czech *et al.*, *ibid.*, p. 1310.
22. H. F. Dovey, S. Suomesaari-Chrysler, I. Lieberburg, S. Hinha, P. S. Kiem, *NeuroReport* **4**, 1039 (1993).
23. To estimate the percentage of long Aβ from the [^{3}H]valine-labeled COOH termini (Fig. 1, C and D), we divided the cpm in fractions with COOH termini from long Aβ by the total cpm in the fractions shown. As pointed out in the text, this calculation assumes, perhaps incorrectly, that the recovery of COOH-termini is the same for $A\beta_{1-40}$ and for longer Aβ. This calculation could not be used to estimate the percentage of long Aβ from the [^{3}H]isoleucine-labeled COOH-termini shown in Fig. 1, E to F, because COOH-termini from $A\beta_{1-40}$ are not labeled by isoleucine. Thus, in this experiment, we first determined the total cpm in the labeled Aβ used as starting material by separating a representative sample by 10 to 16% tris-tricine SDS-PAGE, visualizing 4-kD Aβ in the dried gel, extracting the excised 4-kD band with Solvable (Dupont) according to the manufacturers instructions, and counting. The cpm recovered as COOH-termini from long Aβ (Fig. 1, E to F) were multiplied by a factor of 3 because long COOH-termini have a single isoleucine whereas 4-kD Aβ has three isoleucines, and were used to calculate the percentage of original starting 4-kD Aβ from which long COOH-termini were recovered. With the methods used here, COOH-termini will only be recovered from a fraction of the long Aβ in the original starting material. The values plotted in Fig. 1, E to F, are estimates of the actual percentage of long Aβ in the original starting material calculated by arbitrarily assuming that COOH-termini were recovered from 14% of the long Aβ in the starting material. This reasonable assumption yields values for the percentage of long Aβ that are essentially identical to those obtained by sandwich ELISA. It is evident that the percentage of long Aβ varies considerably depending on the method of estimation used. However, the specific method used to estimate the percentage of long Aβ does not affect our estimate of the shift toward long Aβ produced by the βAPP_{717} mutations because the same method was always used to calculate the percentage of long Aβ produced by cells expressing a suitable control βAPP or the βAPP_{717} mutation to which it was compared.
24. N. Suzuki *et al.*, *J. Biochem.* **113**, 549 (1993).
25. L. Otvos, G. I. Szendrei, V. M.-Y. Lee, H. H. Mantsch, *Eur. J. Biochem.* **211**, 249 (1993).
26. N. Suzuki *et al.*, *J. Immunol. Methods* **118**, 245 (1989).
27. Confluent cells in 10-cm dishes were continuously labeled for 12 hours with [^{35}S]methionine (200 μCi/ml) plus either [^{3}H]valine (200 μCi/ml) or [^{3}H]isoleucine (200 μCi/ml) in 4 ml of minimum essential medium (MEM) that was deficient in the amino acids used for radiolabeling. Radiolabeled Aβ released into the medium was isolated by immunoprecipitation, 10 to 16% tris-tricine SDS-PAGE, and transfer to immobilon as previously described (*13*). After drying, radiolabeled 4-kD Aβ was visualized by autoradiography. The 4-kD Aβ bands were excised, blocked for 30 min at 37°C with 0.5% PVP-40 in 0.1 M acetic acid, and washed at least 10× with deionized water. In each experiment, six immobilon strips containing in aggregate the labeled Aβ released from six dishes of confluent cells were cut into ~1-mm squares and digested for 24 hours in the dark with ~500 μl of 70% formic acid containing 0.05 g of CNBr, 2.0 μg of $A\beta_{36-40}$, and 2.0 μg of $A\beta_{36-42}$. The digestion mixture was dried and extracted with 40% acetonitrile at 37°C for 5 hours and then with 40% acetonitrile with 0.1% trifluoroacetic acid (TFA) for 30 min at 50°C. These extracts were pooled and then dried, and the resultant peptides were brought up in 0.05% TFA. Peptides were then separated by RPLC with a Vydac C4 column (4.6 by 250 mm). Fractions (200 μl) were collected at 1-min intervals, and the radioactivity in each fraction was initially assessed with one-fifth (40 μl) of the fraction. Subsequently, the remainder of each fraction was either counted, sequenced, or radiosequenced as described in the text. Methods for estimating the percentage of long Aβ reported in the text and shown in (E) and (F) are described in (*23*).
28. Sandwich ELISAs were, in general, done as previously described (*25*). BAN-50 was immobilized on 96-well microtiter plates (A/S Nunc, Kamstrup, Denmark) by incubation of 1.0 μg of antibody in 0.1 ml of 0.1 M sodium carbonate buffer (pH 9.6) in each well at 4°C for 1 day. After washing the plate with 0.3 ml of phosphate-buffered saline (PBS) [0.1 M phosphate, 0.15 M NaCl (pH 7.4)], 0.3 ml per well of 1% Block Ace (Snow Brand Milk Products, Sapporo, Japan) in PBS containing 0.05% NaN_3 was added to the plate, and the plate was stored at 4°C until use. Standards were prepared by dilution of stock $A\beta_{1-42}$ prepared as previously described (*24*) or $A\beta_{1-40}$ (Bachem) with buffer EC [0.02 M phosphate buffer (pH 7.0) containing 0.4 M NaCl, 2 mM EDTA, 0.4% Block Ace, 0.2% bovine serum albumin (BSA), 0.05% CHAPS, and 0.05% NaN_3]. These standard solutions or samples to be tested were diluted with buffer EC (0.1 ml) and reacted with a BAN-50–coated microtest plate at 4°C for 48 hours. After being washed three times with PBS, the plate was reacted at 4°C for 24 hours with 0.1 ml of horseradish peroxidase–labeled detector antibody, BA-27, or BC-05 diluted appropriately (1000 or 200 times, respectively) with buffer C [0.02 M phosphate buffer (pH 7.0) containing 0.4 M NaCl, 2 mM EDTA, and 1% BSA]. The plate was again washed four times with PBS, and bound enzyme activity was measured with a substrate solution (0.1 ml) of the TMB microwell peroxidase system (Kirkegaad Perry Lab., Gaithersburg, MD). The enzyme reaction was stopped with 0.1 ml of 1 M phosphoric acid, and absorbance at 450 nm was measured with a microplate reader. $A\beta_{1-40}$ and $A\beta_{1-42}$ were specifically detected by BAN-50/BA-27 and BAN-50/BC-05 ELISAs, respectively, with the detection limits less than 1 fmol per well. Monoclonal antibodies BAN-50, BA-27, and BC-05, were prepared as follows. Synthetic peptides of Cys^{17} $A\beta_{1-16}$ and $Cys^{34}A\beta_{35-43}$ were conjugated with bovine thyroglobulin (BTG) previously maleimidated with N-(maleimidobutyryloxy) succinimide. $A\beta_{1-40}$ was conjugated with BTG with 0.3% glutaraldehyde as a coupling agent. These immunogens (80 μg per mouse), together with complete or incomplete Freund's adjuvant, were subcutaneously injected into BALB/c mice at 3-week intervals. Four days after intravenous injection of 200 μg of immunogen per mouse, splenocytes from each immunized mouse were fused with mouse myeloma cells P3-X63Ag8-U1 as described previously (*26*). Monoclonal antibodies BAN-50, BA-27, and BC-05 were selected from those directed against $A\beta_{1-16}$, $A\beta_{1-40}$, and $A\beta_{35-43}$, respectively. To investigate the epitope of BA-27, we prepared $A\beta_{1-38}$ and $A\beta_{1-39}$ from $A\beta_{1-40}$ by limited proteolysis with carboxypeptidase Y. These peptides were purified by reversed-phase HPLC and characterized by FAB mass spectrometry. In a BAN-50/BA-27 sandwich-ELISA, cross-reactivities with $A\beta_{1-28}$, $A\beta_{1-38}$, $A\beta_{1-39}$ versus $A\beta_{1-40}$ were 0%, 0.7%, and 1.7%, respectively. These results indicate that the major epitope of BA-27 involves the COOH-terminal valine at position 40.
29. We thank C. Kitada, Y. Ishibashi, and T. Kikuchi of Takeda Chemical Industries for peptide synthesis and analysis. Supported by NIH grant AG06656 and an ADRDA Zenith award.

24 January 1994; accepted 4 April 1994